Earth and Planetary Science Letters 455 (2016) 125–139

Contents lists available at ScienceDirect

Earth and Planetary Science Letters

www.elsevier.com/locate/epsl

Refining the Early Devonian time scale using Milankovitch cyclicity in Lochkovian–Pragian sediments (Prague Synform, Czech Republic)

A.C. Da Silva [a,b,*], J. Hladil [c], L. Chadimová [c], L. Slavík [c], F.J. Hilgen [e], O. Bábek [d], M.J. Dekkers [a]

[a] Utrecht University, Department of Earth Sciences, Paleomagnetic Laboratory 'Fort Hoofddijk', Netherlands
[b] Liège University, Sedimentary Petrology Laboratory, Belgium
[c] Czech Academy of Sciences, Institute of Geology, v.v.i., Prague, Czech Republic
[d] Department of Geology, Palacký University, Olomouc, Czech Republic
[e] Utrecht University, Department of Earth Sciences, Stratigraphy & Paleontology, Netherlands

ARTICLE INFO

Article history:
Received 15 March 2016
Received in revised form 1 September 2016
Accepted 3 September 2016
Available online 5 October 2016
Editor: M. Frank

Keywords:
orbital time scale
spectral analysis
Devonian
magnetic susceptibility
gamma ray spectrometry
limestone

ABSTRACT

The Early Devonian geological time scale (base of the Devonian at 418.8 ± 2.9 Myr, Becker et al., 2012) suffers from poor age control, with associated large uncertainties between 2.5 and 4.2 Myr on the stage boundaries. Identifying orbital cycles from sedimentary successions can serve as a very powerful chronometer to test and, where appropriate, improve age models. Here, we focus on the Lochkovian and Pragian, the two lowermost Devonian stages. High-resolution magnetic susceptibility (χ_{in} – 5 to 10 cm sampling interval) and gamma ray spectrometry (GRS – 25 to 50 cm sampling interval) records were gathered from two main limestone sections, Požár-CS (118 m, spanning the Lochkov and Praha Formations) and Pod Barrandovem (174 m; Praha Formation), both in the Czech Republic. An additional section (Branžovy, 65 m, Praha Formation) was sampled for GRS (every 50 cm). The χ_{in} and GRS records are very similar, so χ_{in} variations are driven by variations in the samples' paramagnetic clay mineral content, reflecting changes in detrital input. Therefore, climatic variations are very likely captured in our records.

Multiple spectral analysis and statistical techniques such as: Continuous Wavelet Transform, Evolutive Harmonic Analysis, Multi-taper method and Average Spectral Misfit, were used in concert to reach an optimal astronomical interpretation. The Požár-CS section shows distinctly varying sediment accumulation rates. The Lochkovian (essentially equivalent to the Lochkov Formation (Fm.)) is interpreted to include a total of nineteen 405 kyr eccentricity cycles, constraining its duration to 7.7 ± 2.8 Myr. The Praha Fm. includes fourteen 405 kyr eccentricity cycles in the three sampled sections, while the Pragian Stage only includes about four 405 kyr eccentricity cycles, thus exhibiting durations of 5.7 ± 0.6 Myr and 1.7 ± 0.7 Myr respectively. Because the Lochkov Fm. contains an interval with very low sediment accumulation rate and because the Praha Fm. was cross-validated in three different sections, the uncertainty in the duration of the Lochkov Fm. and the Lochkovian is larger than that of the Praha Fm. and Pragian. The new floating time scales for the Lochkovian and Pragian stages have an unprecedented precision, with reduction in the uncertainty by a factor of 1.7 for the Lochkovian and of ~6 for the Pragian. Furthermore, longer orbital modulation cycles are also identified with periodicities of ~1000 kyr and 2000–2500 kyr.

1. Introduction

A major challenge for improvement of the Devonian Time scale is the limited number of good quality and chronostratigraphically fixed radiometric ages within this period (synthesis in Becker et al., 2012). The error bars of Early Devonian stage boundaries range from 2.5 to 4.2 Myr, and are among the highest of the entire Phanerozoic Geological Time Scale (De Vleeschouwer and Parnell, 2014). An useful approach to improve the Devonian Time scale

* Corresponding author at: Liège University, Sedimentary Petrology Laboratory, Belgium and Utrecht University, Paleomagnetic Laboratory (Fort Hoofddijk), Netherlands.
E-mail addresses: ac.dasilva@ulg.ac.be (A.C. Da Silva), HLADIL@gli.cas.cz (J. Hladil), chadimova@gli.cas.cz (L. Chadimová), slavik@gli.cas.cz (L. Slavík), F.J.Hilgen@uu.nl (F.J. Hilgen), babek@prfnw.upol.cz (O. Bábek), M.J.Dekkers@uu.nl (M.J. Dekkers).

http://dx.doi.org/10.1016/j.epsl.2016.09.009
0012-821X/

would be to identify Milankovich cycles in the sedimentological record, which can be used as powerful chronometers (e.g. Hinnov and Ogg, 2007). The complete interference pattern of these cycles, the astronomical solution, has been theoretically calculated for the Cenozoic (Laskar et al., 2011) and most of the Cenozoic has now been astronomically age calibrated (e.g. Hilgen et al., 2012). These precise orbital solutions are not available for the Paleozoic. However, the 405 kyr eccentricity cycle is known to be very stable (Laskar et al., 2011) and has been used to build floating astronomical time scales for Mesozoic and Palaeozoic successions (e.g. Boulila et al., 2010; De Vleeschouwer et al., 2015). Furthermore, the basic periods of obliquity and precession cycles as a function of age become shorter back in time. This is a consequence of secular deceleration of the Earth's rotation rate, the increase of the distance between Earth and Moon, and the dynamical ellipticity of the Earth (Berger et al., 1992). These eccentricity, obliquity and precession periodicities serve as a template for the identification of orbital frequencies in target sections using spectral analysis. Following pioneering work on Devonian cyclostratigraphy (e.g. Chlupáč, 2000) in which robust spectral techniques are largely absent. More recent efforts in constructing precise floating astronomical time scales have been carried out for the Eifelian (Ellwood et al., 2015), Givetian (De Vleeschouwer et al., 2015), Frasnian (De Vleeschouwer et al., 2012) and the Frasnian–Famennian boundary and topmost Famennian (De Vleeschouwer et al., 2013), leaving the Early Devonian presently uncharted.

The Prague Synform (Czech Republic) is a perfect target for applying cyclostratigraphy to improve the geological time scale of the Early Devonian. It includes the historical stratotypes for the Lochkovian and Pragian stages in continuous deep marine records having not only a well-established biostratigraphy and sedimentological context but also an extensive database of high resolution magnetic susceptibility (χ_{in}) and gamma ray spectrometry (GRS) records (see Table 1A for references). χ_{in} and GRS have classically been used as proxies for detrital input and therefore, as a proxy for climatic changes (e.g. Mayer and Appel, 1999; Kodama and Hinnov, 2015; Kodama et al., 2010; Boulila et al., 2010; Hinnov et al., 2013; Da Silva et al., 2013; De Vleeschouwer et al., 2015). In this paper, we search for orbital cyclicity in different target sections, using χ_{in} and GRS records, with the aim to improve the Lochkovian and Pragian time scale.

2. Geological setting and target sections

The selected sections (Požár-CS, Pod Barrandovem and Branžovy) are all from the Prague Synform, formed during the Variscan orogeny. The original sedimentary basin was located at about 20° to 35° southern latitude (Fig. 1A), within the Rheic Ocean, and was part of the North Gondwana Province (Plusquellec and Hladil, 1998). The Lochkovian was characterized by extreme greenhouse climate, with average low latitude sea surface water temperatures (SST) around 30–32 °C calculated from oxygen isotopes in apatite from conodonts (Joachimski et al., 2009). Average SSTs start to decrease in the early Pragian and show minimum values around 22 °C in the late Emsian to Givetian (Joachimski et al., 2009). Early Pragian times were still relatively hot and humid while major climatic instability characterized mid to late Pragian times (Slavík et al., 2016).

The historical stratotypes for the Lochkovian and Pragian were defined in the Czech Republic, in the Prague Synform. The Lochkovian, in its most recent definition (Becker et al., 2012) is equivalent to its historical definition and roughly corresponds to the Lochkov Formation (Fig. 2). The historical Pragian is more or less equivalent to the Praha Fm, but the Pragian has been redefined a few decades ago (based on the basal Emsian GSSP in Kitab, Uzbekistan). It has become significantly shorter: it now corresponds only to a relatively small portion of the lower Praha Fm. (Fig. 2). However, this definition has been strongly criticized (Slavík et al., 2007; Carls et al., 2008) and a new definition of the Pragian is in progress (SDS Newsletter, 2014, p. 14). For this reason we also consider the duration of the Lochkov and Praha Fms., because their biostratigraphy is very well documented and they are still used as references (e.g. Becker et al., 2012).

During the Devonian, the Prague Basin was affected by active faulting, leading to the creation of local submarine highs, and thus to substantial difference in sediment thickness between relatively closely spaced sections (Chlupáč et al., 1998). Indeed, the Praha Fm. in the Požár-CS section is much shorter than in Pod Barrandovem, which is located only 5 km east of Požár-CS (Praha Fm. is 40.4 m thick in Požár-CS, while the same formation reaches ~174 m thickness in the Pod Barrandovem section, to which ~10 m missing at the base should be added to complete the Praha Fm.). However, facies in both sections are relatively similar, being dominated by carbonate distal off-shore facies. The rhythmically deposited, slightly clayey off-shore limestones are mostly hemipelagites and calciturbidites, deposited in an oxygenated water column (Hladil et al., 2010).

The continuity – crucial for a meaningful application of spectral methodology – of the different sections studied has been assessed in the literature, through biostratigraphy, sedimentary petrology and geophysical methods. The Lochkov and Praha Fms. in the Požár-CS section are partly condensed, but also considered as essentially complete without significant gaps (Koptíková et al., 2010a; Slavík, 2004a; Slavík et al., 2012). In the Branžovy section, a similar lithological succession as at Požár-CS is observed, but with a different thickness and with potential sedimentary reworking (Slavík, 2004a). The Praha Fm. at Pod Barrandovem is considered as nearly complete and undisturbed (Chlupáč, 2000), with the exception of a relatively short interval at the very base of the Praha Fm., where ~10 m of the Slivenec limestones is missing (Fig. 2). Furthermore, there is potentially a gap at the contact with the overlying Zlichov Fm.; where the duration of this gap is unknown but very likely short as all conodont zones are present (Slavík, 2004a).

The cyclicity of these deposits has already been studied by Chlupáč (2000), who identified ~410–450 bedding couplets within the Lochkovian and estimated about 350 to 380 couplets within the historical Pragian, pointing to a longer duration of the Lochkovian compared to the historical Pragian.

3. Materials and methods

3.1. Selected sections and sampling intervals

Two main sections Požár-CS and Pod Barrandovem were selected, with the highest sampling rate and with both χ_{in} and GRS records, complemented by one extra section (Branžovy) with a lower sampling rate GRS record. The locations of the different sections are shown on Fig. 1; Požár-CS is a composite section of Požár-1 and Požár-3 (Fig. 1E, Table A1). Sampling intervals vary between one sample every 5, 10, 25 and 50 cm (Table A1).

3.2. Magnetic measurements

Magnetic susceptibility (χ_{in}) measurements have been carried out in different laboratories but all on similar devices, using a KLY-2 at the Czech Academy of Sciences, a KLY-3 at Liège University, and a MFK-1 at Utrecht University, which are essentially different generations of the same type of Kappabridge device, manufactured by AGICO (Brno, Czech Republic). χ_{in} is mass-specific, in m^3/kg. Some hysteresis data were also gathered to get insight into the origin of the magnetic minerals carrying the magnetic susceptibility signal (detailed methodology in Appendix 1).

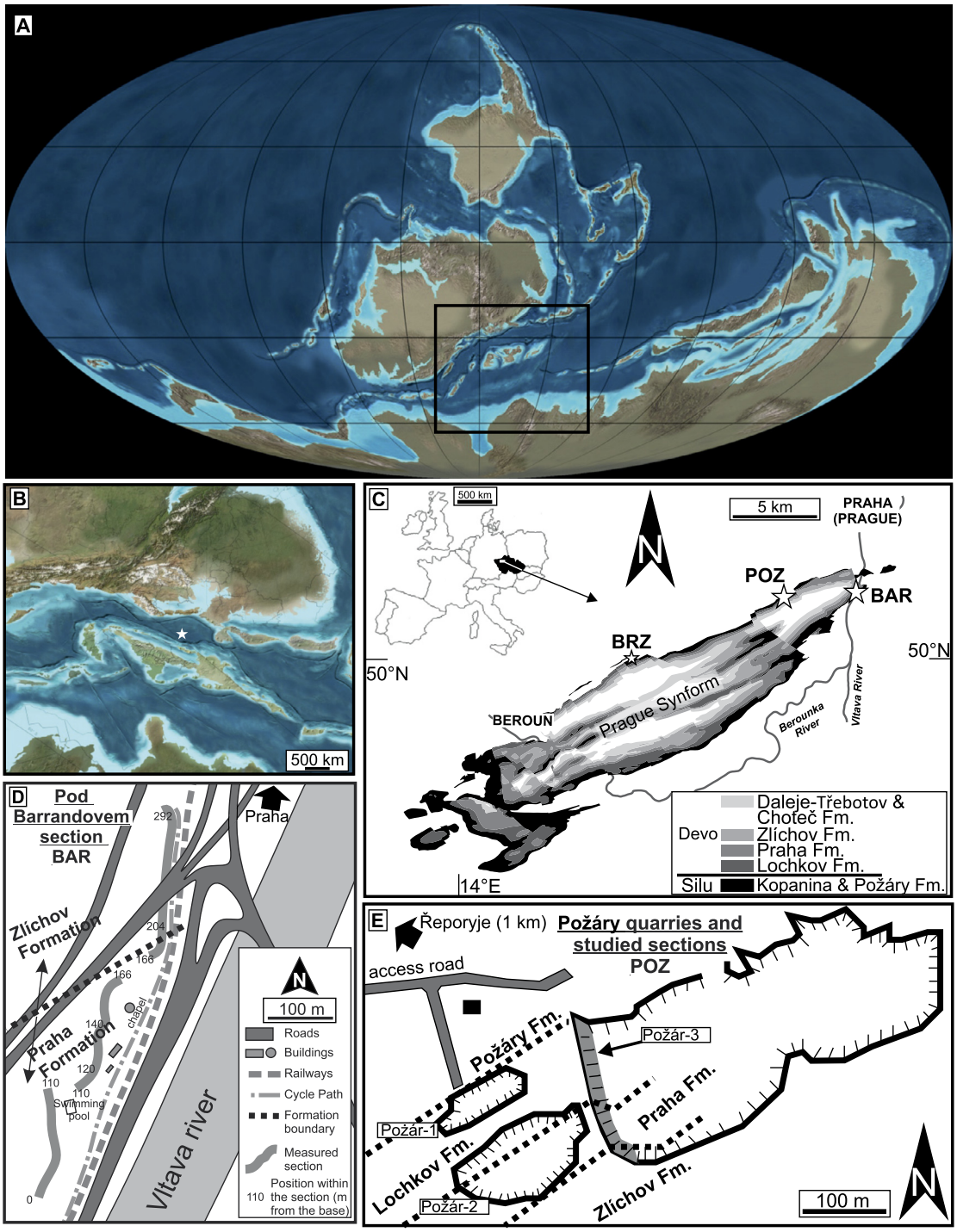

Fig. 1. Geological setting of the Prague Synform and studied sections. (A) Early Devonian (400 Myr) palaeogeographic reconstruction, after R. Blakey, Colorado Plateau Geosystems http://cpgeosystems.com/. The rectangle corresponds to the zone with more detailed palaeogeography in 1B (1B slightly rotated with respect to 1A). (B) Detailed early Devonian palaeogeographic maps, the star corresponds to the location of the Prague Synform, same source as 1A. (C) Location of Czech Republic and of the Prague Synform, geological map and location of the different sections (BRZ = Branžovy, POZ = Požár-CS, BAR = Pod Barrandovem). Devo = Devonian and Silu = Silurian. (D) Pod Barrandovem section, precise location, formations and sampling trajectories (the Zlichov Fm. is not discussed here). (E) Požár-CS section (Požár-1 + Požár-3), precise location, formations and location of Požár-1, Požár-2 and Požár-3 quarries.

3.3. Gamma ray spectrometry

GRS measurements are related to the abundance of the three most important radioactive elements occurring in sedimentary rocks, K, Th and U. For carbonate strata, K and Th are classically interpreted as reflecting clastic content, whereas U is determined by diagenetic processes involving changes in oxidation state. GRS for Požár-CS and Pod Barrandovem was measured using a GR-320 enviSPEC portable spectrometer (detailed methodology in Koptíková et al., 2010a). GRS for Branžovy was measured using an RS-230 Super Spec portable spectrometer (Radiation Solutions, Inc., Canada; details in Bábek et al., 2013). Here we focus on K and Th records. Counts per second in selected energy windows were converted by the instrument to concentrations of K (%) and Th (ppm), based on calibrations carried out by the manufacturer.

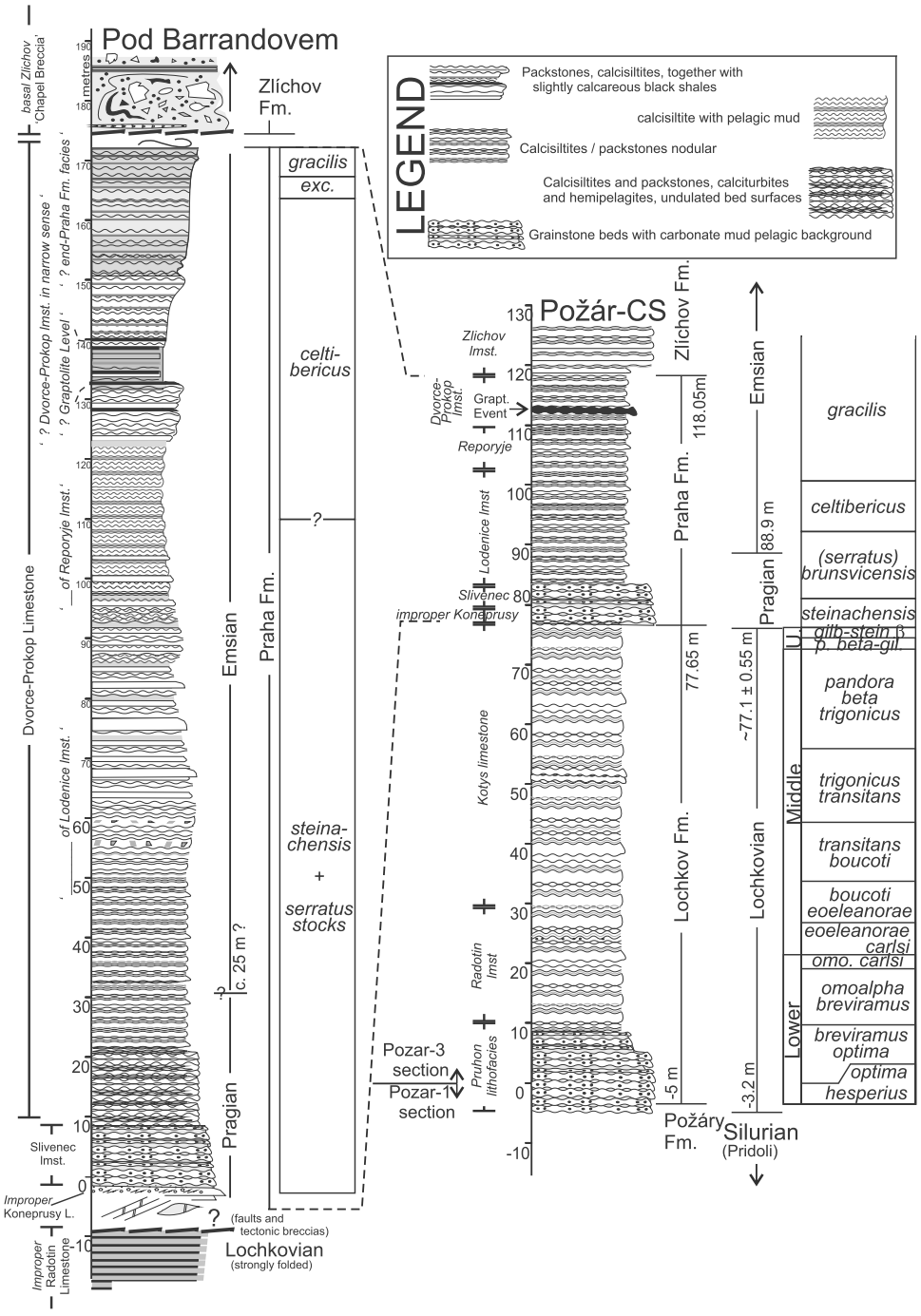

Fig. 2. Lithological column, formations, members and stages in the Pod Barrandovem and Požár-CS sections. Conodont zonations for the Lochkovian of the Požár-CS section are from Slavík et al. (2012). Zonations for the Praha Formation in that section and in the Pod Barrandovem section are from Slavík (2004a, 2004b) and Slavík et al. (2007). Lithological columns have been modified and harmonized from Koptíková et al. (2010a, 2010b), Hladil et al. (2010, 2011) and Vacek et al. (2010) (see also Table A1). Abbreviations: Grapt. Event = Graptolite Event, Fm. = Formation, lmst = limestone, U. = Upper.

3.4. Spectral analysis techniques

All the χ_{in} and GRS data were linearly interpolated onto evenly spaced samples records and detrended (linear detrending) prior to any spectral analysis. The Continuous Wavelet Transform (CWT) of Torrence and Compo (1998) was employed, using a Morlet wavelet, and run on a MATLAB platform. Interpolation, detrending, Evolutive Harmonic Analysis (EHA, Meyers et al., 2001), the Multi-Taper Method (MTM) and MTM-harmonic test (F-test) developed by Thomson (1982), Average Spectral Misfit (ASM, Meyers and Sageman, 2007), tuning and band-pass filtering, as well as the Hilbert transform have all been performed with the "Astrochron" package, the open source R package developed by Meyers (2014).

The complete analytical protocol is as followed:

As a first step, two independent evolutive spectral techniques (also referred to as Evolutionary Spectrogram in Kodama and Hinnov, 2015) CWT and EHA were applied to χ_{in} (highest sampling resolution) and the logarithmic GRS records to reveal the evolution of periodicities for the studied sections and also to detect changes in cycle thickness and, hence, sediment accumulation rate (SAR). By using the logarithmic signal, the strong amplitude fluctuations within these GRS lower resolution signals were removed.

Table 1
Požár-CS and Pod Barrandovem sections with subdivision of stratigraphic intervals into portions of constant sediment accumulation rate (SAR), with arguments for subdivision. (1) Stratigraphic interval (in m) considered as deposited with constant SAR. (2) CWT (Continuous Wavelet Transform) and EHA (Evolutive spectral analysis): V = the change of SAR is visible in the CWT and/or EHA. (3) Lithology = Lithological changes associated with the subdivision and respective members. Lmst = limestone. (4) Condensed: arguments for intervals considered condensed.

(1) Požár-CS	(2) CWT-Eha	(3) Lithology	(4) Condensed
−5 to 12 m	V	Pruhon lithofacies – crinoidal limestone, 2–5 cm beds	
12–50 m	V	Radotin lmst. – Kotys lmst. 2–10 cm beds	
50–70.8 m	V	Kotys lmst. – Alternation massive and thin beds	
70.8–78 m	Not clear	Kotys limestone – Koneprusy	Late Lochkovian biostratigraphically very condensed (Slavík et al., 2012)
78–112 m	V	Slivenec, Lodenice, Reporyje members – graptolite interval	
112–118 m	V	Dvorce-Prokop limestone	Dvorce-Prokop limestone condensed (Hladil et al., 2010)
(1) Pod Barrandovem	(2) CWT-Eha	(3) Lithology	(4) Condensed
0–12 m	V	Slivenec Lmst	
12–55 m	V	Lodenice Lmst (thin beds)	
55–92 m	V	Lodenice Lmst (thicker beds)	
92–176 m	V	Reporyje Lmst	

By combining the results from CWT and EHA with the sedimentological observations (mostly the subdivision into Members) and published conodont data, the Požár-CS and Pod Barrandovem sections were divided into intervals with relatively constant SAR (Table 1). For each of these intervals, we subsequently performed MTM analysis, with its associated F-test using three tapers and we extracted frequencies that reached 95% confidence level (CL). These frequencies were implemented into the ASM package. Very similar frequencies are combined to their average value, considering that these slightly different frequencies are probably only due to small changes in SAR. The ASM technique, developed by Meyers and Sageman (2007), compares the frequencies obtained through spectral analysis with the orbital frequencies and computes the SAR that provides the best fit, with the highest confidence level. It also includes an explicit statistical test for rejection of the null hypothesis of no orbital forcing (Ho_SL). The target orbital frequencies for the Lochkovian and Pragian used in the ASM are based on Berger et al. (1992). The SARs obtained by ASM are compared with those obtained by CWT and EHA. All SARs (in cm/kyr) in this paper are post compaction.

To remove the impact of the changes in SAR, χ_{in} records of Pod Barrandovem and Požár-CS and the GRS-Th record of Branžovy were tuned, constructing a floating astrochronology for the Lochkovian and Pragian. The tuning was performed through the selection of multiple tie-points, related to the 405 kyr cycles, to track frequency drift and take short-term changes in SAR into account (commands in Astrochron: trackFreq, freq2sedrate, sedrate2time and tune). This resulted in a tuned composite section in the time domain, instead of the stratigraphic domain. The tuned records are then band-pass filtered, with a cosine-tapered window, to extract the 100 kyr and 405 kyr eccentricity cycles. We studied the low frequency part of the MTM tuned composite records to determine the amplitude modulation of the eccentricity related cycles and to detect cycles with a long (>405 kyr) period (following the methodology of Fang et al., 2015). In addition, the amplitude modulation of the filtered 100 kyr and 405 kyr cycles was extracted for each section using the Hilbert Transform, which is used to find the enveloping curve of the bandpass filtered signal. MTM was performed on the resultant amplitude modulation curve.

4. Results – spectral analysis of χ_{in} and GRS records

Barrandovem and Požár-CS sections were subdivided into portions with a constant SAR (arguments for subdivision in Table 1). MTM and ASM analyses were performed on each of these intervals on χ_{in}, and results were compared with the EHA (χ_{in}, GRS) and CWT (χ_{in}) results of the records of Pod Barrandovem, Požár-CS and Branžovy. In most cases, results from all spectral techniques are supporting each other, pointing to a similar SAR. In those cases, the interpretation is straightforward and this was the case for the different intervals in Pod Barrandovem and Branžovy sections, as well as for 3 intervals out of 6 in Požár-CS. When the results from ASM and CWT and EHA are not supporting each other (3 intervals out of 6 in Požár-CS), the following approach is adopted (and is detailed in section 4.1): (a) when the results obtained with ASM are not coherent with the results obtained with CWT and EHA (intervals 12–50 m and 78–112 m): for these two intervals, there is a high number of frequencies calculated by the MTM and F-test (Fig. 3 and Fig. A1). This high number of frequencies is due to a variable SAR, which would lead to a single orbital cycle represented by multiple frequencies or periods (or cycle thickness). In these two cases, CWT and EHA yielded similar results, so the ASM results were discarded in favor of the results calculated by the CWT and EHA. (b) in interval 70.8–78 m from Požár-CS, the results from CWT or EHA were not clear and couldn't be used to support the ASM results. In this case, we consider the ASM results robust, as they are supported by other, more qualitative arguments, such as biostratigraphic and sedimentologic information (Table 1).

4.1. Požár-CS section (Figs. 3–A3 and A1)

It is necessary to define potential extreme SARs for each section segment before running Average Spectral Misfit. For Požár-CS, as the Lochkovian is about 82 m long and lasts 8.4 Myr (Becker et al., 2012) or 7.7 Myr (De Vleeschouwer and Parnell, 2014), with an uncertainty of ±3.2 Myr (Becker et al., 2012) or ±2.9 Myr (De Vleeschouwer and Parnell, 2014) for the Pridoli–Lochkovian boundary, and ±2.8 Myr (Becker et al., 2012) or ±3.5 Myr (De Vleeschouwer and Parnell, 2014) for the Lochkovian–Pragian boundary. Possible durations stretch between 4.5 and 11.4 Myr, which corresponds to SARs between 0.7 cm/kyr to 1.8 cm/kyr. We selected even larger SARs between 0.1 and 3 cm/kyr, for the Lochkovian, to allow for larger variations in SAR, noting that certain portions of the section are condensed. Based on the same considerations, similar SARs are used for the Pragian in Požár-CS.

For the −5 to 12 m interval, results are consistent for the different techniques used (CWT, ASM) and for the different records (χ_{in}, GRS-Th, GRS-K), and all point to a similar interpretation (Figs. 3 and A3). A SAR of 1.0 cm/kyr was obtained with ASM, with 4.1% Ho_SL, in other words, there is 4.1% probability that this ASM value could be derived by chance. With this interpretation, the strong power band in the EHA or CWT with a frequency of 0.25 m^{-1} or a period of 4 m (Table A2) is linked to the 405 kyr eccentricity (also called E1, Figs. 3 and A3).

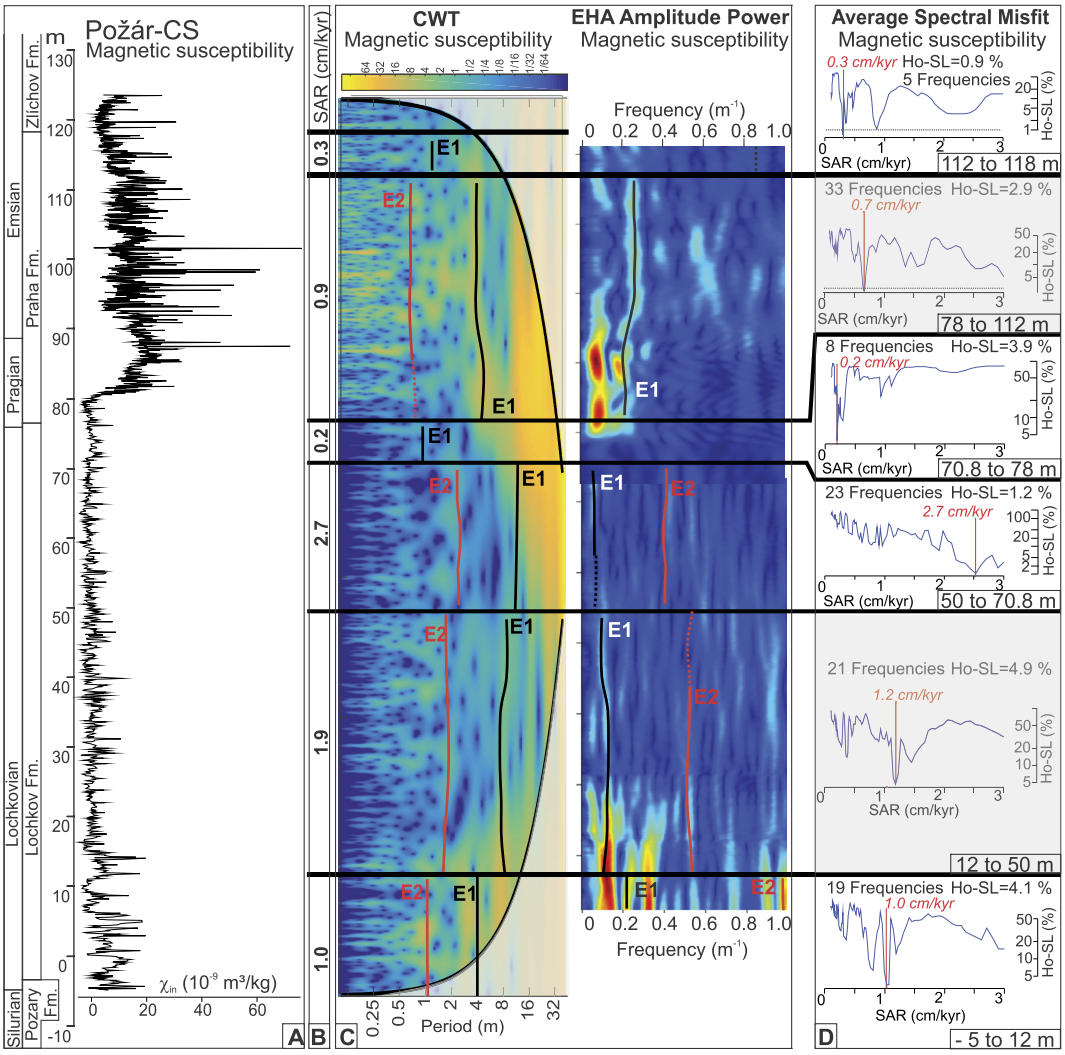

Fig. 3. Požár-CS section (Lochkov and Praha Formations) with spectral analysis of magnetic susceptibility (χ_{in}) records. (A) Stages, formations and χ_{in} record. (B) SAR (cm/kyr) = sediment accumulation rate in cm/kyr, deduced by the combination of sedimentological and palaeontological information with the different spectral and statistical techniques: Continuous Wavelet Transform (CWT), Evolutive Harmonic Analysis (EHA), and Average Spectral Misfit (ASM). Note: when the ASM plot (panel D) is in light grey, the ASM results were not considered further. The Zlichov Fm. is not discussed here. (C) Continuous Wavelet Transform (CWT) and Evolutive Harmonic Analysis (EHA) of the χ_{in}. CWT and EHA include the interpretation of the 405 kyr eccentricity cycles (E1) and 100 kyr eccentricity cycles (E2) (in continuous lines when clear and dotted when extrapolated). (D) Average Spectral Misfit (ASM): the frequencies reaching 95% confidence level in MTM and F-test (Figs. A1–A2) are inputted into the ASM. The optimal SAR in cm/kyr from the ASM is given in red and corresponds to the SAR with the lowest null hypothesis significance level (Ho_SL%). The number of input frequencies into the ASM, obtained from MTM and F-test is also mentioned (X Frequencies in panel D), as well as the optimal Ho_SL (%) from its output. Cf. main text section 4.1. for complete information and interpretations. (For interpretation of the references to color in this figure, the reader is referred to the web version of this article.)

For the 12 to 50 m interval, the ASM indicates an optimal SAR of 1.2 cm/kyr (4.9% Ho_SL). This would result in 5 m cycles (or 0.2 m^{-1} frequency) for the 405 kyr eccentricity E1. However, neither the CWT nor EHA reveal enhanced power at this period or frequency (Figs. 3 and A3). The MTM and F-test combined produce 28 frequencies reaching 95% CL (Confidence Level, Fig. A1), which points to an SAR that may not be stable. This changing SAR is indeed observed in the CWT and EHA (Figs. 3 and A3). As mentioned before, this non-stable SAR makes it problematic to apply ASM. Therefore, the ASM results were discarded in favor of the CWT and EHA results obtained from on the χ_{in} and GRS records. In the CWT and EHA, strong bands are present at a period of ~8 m or at a frequency of 0.13 m^{-1} (Table A2, Figs. 3–A3), that indicate an SAR of 1.9 cm/kyr. The 50 to 70.8 m interval is again characterized by a good fit between all spectral methods, resulting in a straightforward interpretation with an SAR of 2.7 cm/kyr (E1 = ~11 m, Table A2, Figs. 3–A3).

The 70.8–78 m interval is difficult to interpret. As indicated in Table 1, this interval is highly condensed. There appears to be no clear outcome in the CWT and EHA, with strongly undulating results that are usually indicative of perturbations induced by SAR changes. The ASM indicates a very low SAR of 0.2 cm/kyr (3.9 Ho_SL%), corresponding to a 405 kyr eccentricity-related cycle of 0.8 m. The interpretation of this cycle reflecting an orbital imprint with a SAR of 0.2 cm/kyr has a significance of 96.1%. As we know that the SAR in this interval is low (Table 1), we decided to use the ASM results, even though there is no validation from the other techniques. This is a very low SAR; however, we have to keep in mind that it is a post-compaction SAR. Furthermore, these low SARs are not uncommon in similar hemipelagic settings: for example a SAR between 0.04 and 0.7 cm/kyr was found in Upper Devonian and Lower Carboniferous sections from Moravia, Carnic Alps, Rhenish Massif, Montagne Noire, and Pyrenees (Bábek et al., 2016) and a SAR around 0.5 cm/kyr was found in Miocene sediments (affected by a relatively low compaction) from IODP site U1438 (Arculus et al., 2015).

For the 78 to 112 m interval the ASM results in a SAR of 0.7 cm/kyr (2.9 Ho_SL%) which would correspond to a 405 kyr

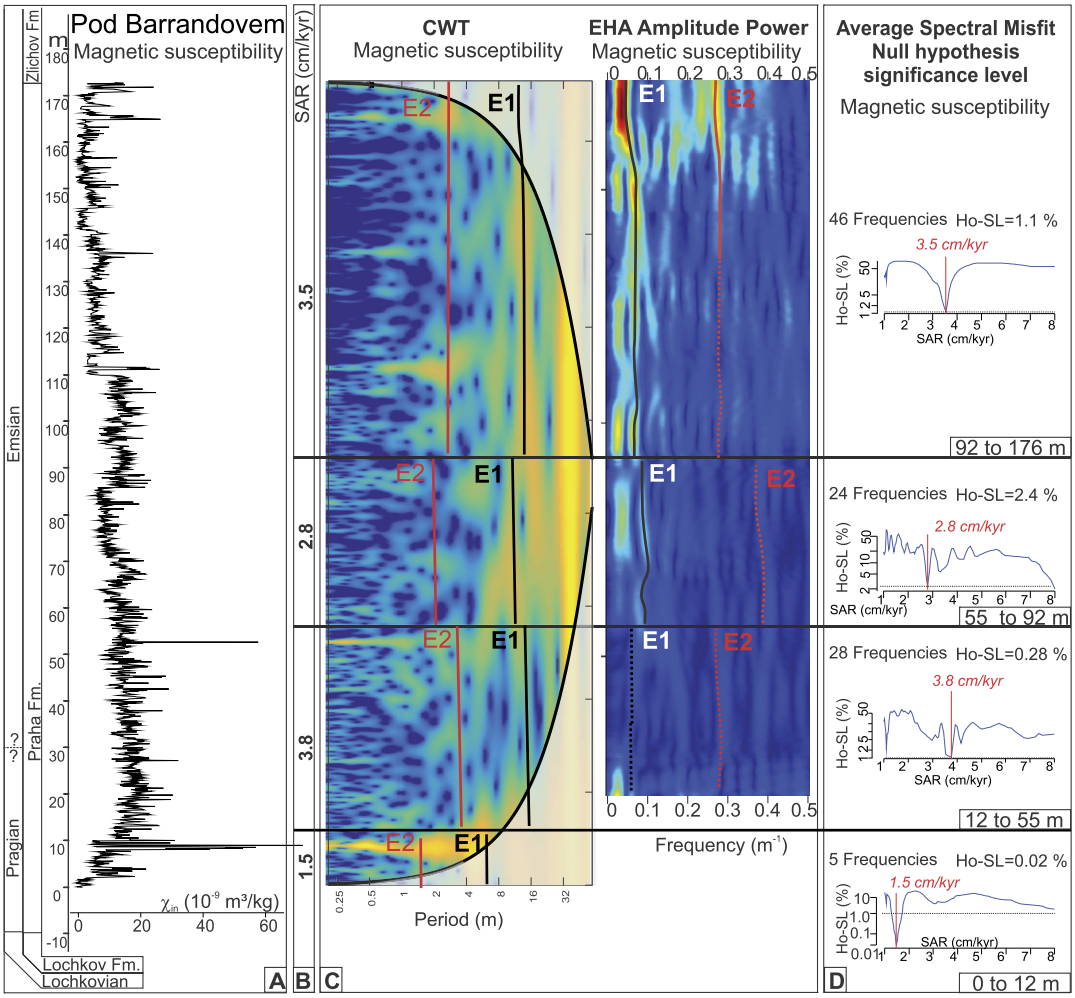

Fig. 4. Pod Barrandovem section (Praha Formation) spectral analysis of magnetic susceptibility (χ_{in})**.** Cf. caption of Fig. 3 for symbol explanation and main text (section 4.2) for more information. (For interpretation of the references to color in this figure, the reader is referred to the web version of this article.)

eccentricity related cycle of 2.8 m, but this result is not present in the CWT or the EHA data. As for the 12 to 50 m interval, the MTM and F-test lead to a very large number of frequencies (43), pointing to a variable SAR. Indeed, the SAR seems to be somewhat higher in the first 10 m of the interval (cf. CWT and EHA of the χ_{in} record, Figs. 3–A3). For this reason, and because the results of CWT and EHA are consistent with each other for the χ_{in} record (Fig. 3), but less clear for the GRS records (Fig. A3) we discard the results from ASM and favor those from EHA and CWT. EHA and CWT are showing a strong band at a period of ~4 m or a frequency of 0.25 m^{-1} and this corresponds to a SAR of 0.9 cm/kyr for this interval (Figs. 3–A3, Table A2).

Within the uppermost 112 to 118 m interval there is an evident change in SAR compared to the previous interval as indicated by the CWT, with the observed shift of the yellow band, indicating a trend toward a lower SAR (Fig. 3A, not seen in the EHA, as this interval is at the end of the record). The ASM results point to a low SAR of 0.3 cm/kyr, with a Ho_SL of 0.9%. This interval was also known as being deposited with a low SAR (Table 1). The SAR of 0.3 cm/kyr is therefore considered robust (E1 = 1.2 m, Fig. 3 and Table A2).

4.2. Pod Barrandovem section (Figs. 4–A4 and A2)

At Pod Barrandovem, the Praha Fm. is about 180 m thick, this would allow SARs between 1 and 8 cm/kyr when applying ASM. The Pod Barrandovem section appears to feature a more stable SAR than the Požár-CS section (compare the stability of the main bands within the CWT and EHA in Figs. 3–A3 and 4–A4). Four intervals of constant SAR have been distinguished (Table 2). The interpretation of orbital cycles in terms of SAR for each interval is straightforward. Indeed, all techniques (CWT, EHA and ASM) and records (χ_{in} and GRS) produce consistent results, leading to a similar interpretation per interval. The position of the 405 kyr eccentricity (E1) and 100 kyr eccentricity (E2) cycles associated with the inferred SAR obtained through ASM invariably fits with a strongly enhanced power band (or an interrupted band for E2) in the CWT of χ_{in} (Fig. 4) and the EHA of χ_{in} and GRS (Figs. 4–A4 and Table A2). The interpretation for each interval is indicated on Figs. 4–A4 and the SAR evolves from 1.5 (between 0–12 m), 3.8 (12–55 m), 2.8 (55–92 m) to 3.5 (92–176 m) cm/kyr.

4.3. Branžovy section

The SAR seems relatively stable in the Branžovy section (see Fig. 5 for the CWT and EHA of the Log GRS-Th record), even with a clear trend toward lower SAR at the top. This trend coincides with a transition between two lithological intervals: 20 to 35 m characterized by crinoidal calcarenites and 39 to 90 m characterized by pelagic nodular calcilutites. An SAR of 1.5 cm/kyr is obtained if we perform an ASM on the entire record, however with Ho_SL of only 16%. This SAR fits with a strong power band at around ~6 m (or a frequency around 0.17 m^{-1}); which would correspond to 405 kyr eccentricity (E1) in the CWT (or in the EHA, Fig. 5). The SAR, de-

Table 2
Duration and uncertainty on the Lochkovian, Lochkov Fm., Pragian and Praha Fm. obtained in this paper and comparison with recently published results (Becker et al., 2012 and De Vleeschouwer and Parnell, 2014). This work: Number of 405 cycles = Number of 405 kyr cycles counted in the Lochkovian, Lochkov Fm., Pragian and Praha Fm. Uncertainty on the position of the boundary (for further explanation, see sections 5.3–5.4. in the main text). Total: combined uncertainty from the lower and upper boundaries; b. = boundary; Lochko. = Lochkovian. Uncertainty on counting E1 cycles (405 kyr), converted into Myr: Lochkovian and Lochkov Fm – high uncertainty on cycle counting related to the occurrence of very low SAR interval within the Lochkov Fm., and because the results are derived from only one section. Pragian and Praha Fm. – low uncertainty on cycle counting because all the techniques and proxies in this interval were pointing to similar results and because these results were also cross-validated over three different sections. Previously published durations and uncertainties.*

	This work: durations and uncertainties				Previously published durations and uncertainties*	
	Number of 405 cycles	Uncertainty		Duration ± uncertainty (Myr)	Becker et al., 2012	De Vleeschouwer and Parnell, 2014
		Position of the boundary (Myr)	Counting E1 cycles			
Pragian	~4	Pragian–Emsian: ±0.02 Lochko.–Pragian: ±0.3 Total: ±0.32	0.4 Myr (1 cycle)	1.7 ± 0.7	3.2 ± 3.8 Myr	3.2 ± 4.3 Myr
Praha Fm.	14	Upper b.: ±0.07 Lower b.: ±0.1 Total: ±0.17	0.4 Myr (1 cycle)	5.7 ± 0.6	–	–
Lochkovian	19	Lochko.–Pragian: ±0.3 Pridoli–Lochko.: ±0.03 Total: ±0.33	2.4 Myr (6 cycles)	7.7 ± 2.8	8.4 ± 4.3 Myr	7.7 ± 4.4 Myr
Lochkov Fm.	19	Upper b.: ±0.1 Lower b.: ±0.02 Total: ±0.12	2.4 Myr (6 cycles)	7.7 ± 2.6	–	–

* Uncertainties are calculated by error propagation of the uncertainties on the lower and upper stage boundaries (see also section 5.4.).

duced from the CWT and EHA and the evolution of the main band between 5 and 7 m, and reflected by the aforementioned change in lithology, is probably varying through time, leading to the relatively poor Ho_SL obtained with ASM.

4.4. Long period cycles

The CWT and EHA of the three studied sections also suggest the presence of cycles with periods longer than 405 kyr (Figs. 3–6). The main low frequencies extracted from the tuned records of the three sections (Fig. 6) correspond to periods of ~1000, ~1300, 2000–2500 and ~4000 kyr. The amplitude envelope of the 405 kyr from Pod Barrandovem reveals a very strong spectral band in MTM between ~1500 and ~5000 kyr while the F-test peaks are recorded at periods of 583, 875, 1050, 2070 and 4268 kyr. For the Požár-CS section, there is also a large spectral peak in MTM between ~1000 and ~5000 kyr but no corresponding peak is observed in the F-test. For Branžovy, there is again a large spectral band for MTM between ~1500 and ~5000 kyr and a single F-test peak at 1135 kyr. The amplitude envelope of the filtered 100 kyr eccentricity related cycle reveals undifferentiated continuous high power in the MTM of both Pod Barrandovem and Branžovy. These are found in combination with F-test peaks at 593 kyr for Požár-CS and at ~540, 765, ~1300 and 1760 kyr for Branžovy.

5. Interpretation

It is important to keep in mind when constructing a high-resolution cylostratigraphic age model that the recording of Milankovitch type of cyclicity in the stratigraphic domain can be altered by different mechanisms, which will produce noise. The processes responsible for producing the noise are (Meyers et al., 2008): the primary response of the climate system to Milankovitch-forced insolation changes, the distortion through the proxy fidelity and diagenetic alteration of the proxy, the response of the depositional environment to climate, including changes in SAR, the sampling protocol and the analytical error associated with the measurement of the proxy.

Concerning the proxy fidelity, we selected χ_{in} as our main proxy and GRS as a secondary proxy. Both proxies have been extensively used to detect paleoclimatic cycles (see Kodama and Hinnov, 2015 and references therein). The impact of diagenesis in potentially altering the primary climatic information reflected in both proxies is, however, typically under-estimated (Riquier et al., 2010; Da Silva et al., 2012, 2013). We will discuss this impact and the fidelity of our proxies in section 5.1. In this research, we selected sections from pelagic and hemi-pelagic settings, which provide superior continuity and the best chances for detecting a meaningful orbital signal with a low degree of distortion (e.g. Hinnov and Ogg, 2007). However, the studied sections also contain calciturbidites and storm deposits, which are classically considered as random (in time) depositional events (Hinnov and Ogg, 2007). The quality of this depositional system as a recorder of orbital cycles will be assessed in section 5.2.

Concerning the sampling protocol and the analytical error, Meyers et al. (2008) emphasize that the analytical error must be small relative to the signal variability, while the duration of the record should be long enough and the sample frequency high enough to resolve the orbital signal and avoid aliasing. In our case, we have selected long sections that cover two entire stages and span several millions of years, using a high sampling density of one sample every 5 or 10 cm for χ_{in} and 25 to 50 cm for GRS (Table A1). Since the SAR varies over the various sections (Fig. 3–4; Table A2), the maximum resolvable frequency, the Nyquist frequency (each cycle must be sampled at least twice), is varying as well. This frequency is tabulated in Table A2, along with the smallest resolvable orbital cycle.

5.1. Origin of the magnetic susceptibility signal and its use for cyclostratigraphy

The entire Palaeozoic sedimentary succession of the Bohemian Massif, including the Prague Synform, was affected by late Variscan remagnetization, which led to the formation of new magnetic minerals (Krs et al., 2001; Grabowski et al., 2010), mostly magnetite (Zwing, 2003). It is thus important to discuss the origin of the magnetic minerals that carry the χ_{in} signal. In earlier cyclostratigraphic or paleoclimatic studies on Palaeozoic remagnetized limestones (e.g. Riquier et al., 2010; Da Silva et al., 2012, 2013; De Vleeschouwer et al., 2012), it was already shown that magnetic susceptibility can still carry an orbital signal despite the remagnetization. A high correlation between χ_{in} and elements commonly interpreted as proxies for detrital input (Al, Si, Ti and Zr) supported the interpretation of χ_{in} reflecting depositional information.

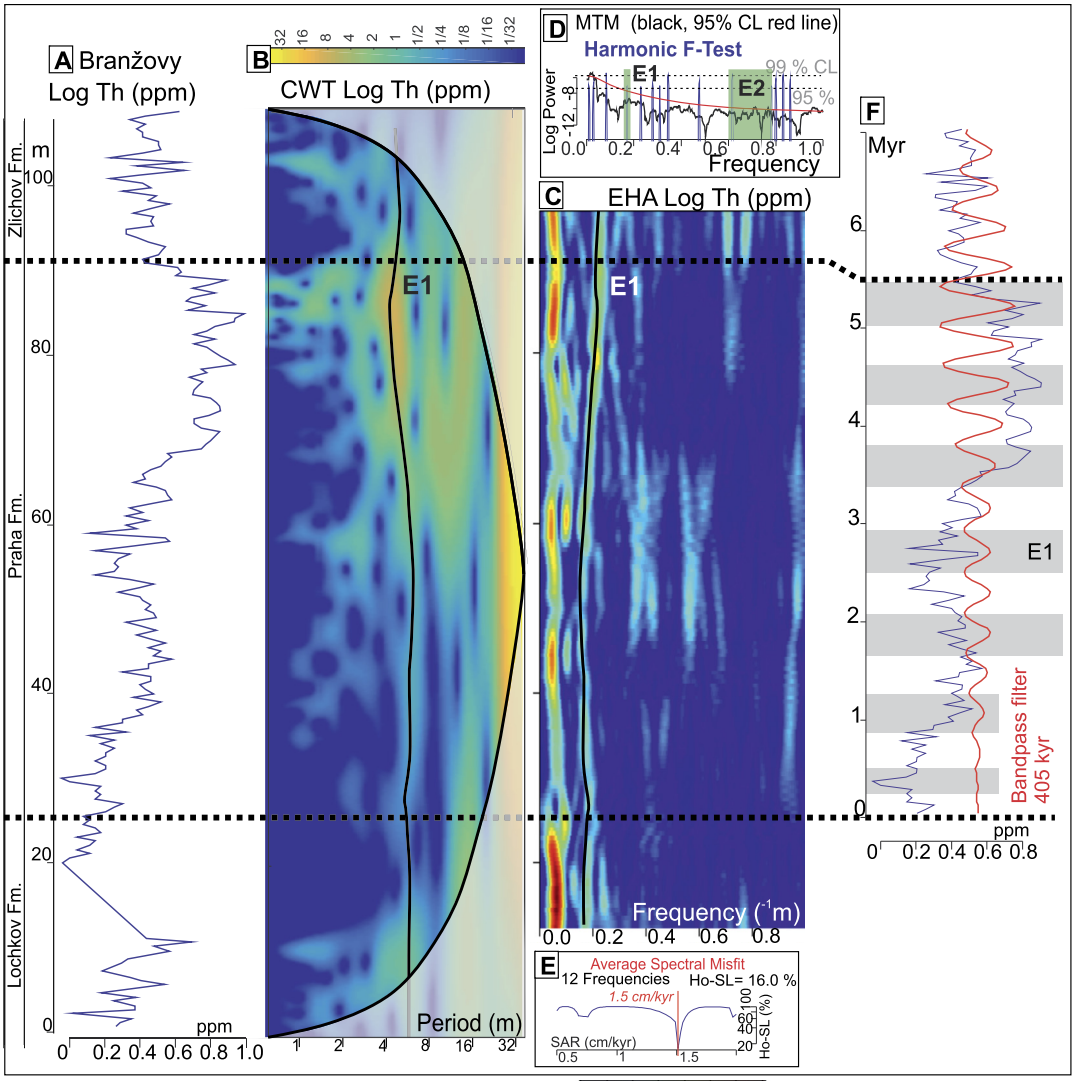

Fig. 5. Spectral analysis of the Log GRS-Th signal from the Branžovy sections (Praha Formation). (A) Log GRS-Th signal in the distance domain and its (B) CWT and interpretation of 405 kyr E1. (C) EHA of the Log-Th signal from Branžovy and interpretation of E1. (D) MTM spectrum (MTM and F-test), with interpretation of the position of the eccentricity cycles (E1 = 405 kyr cycle and E2 = 91–126 kyr cycles). (E) Average Spectral Misfit performed with the frequencies reaching 95% CL in the MTM and F-test (12 frequencies, from 5D) and corresponding null hypothesis significance level (Ho_SL%). (F) Log GRS-Th signal in the time domain and its bandpass filter (405 kyr – E1 – indicated by the alternating grey and white bands). (For interpretation of the references to color in this figure, the reader is referred to the web version of this article.)

In the case of the Pragian limestones, the amount of magnetic minerals produced during remagnetization is considered to be small (Zwing, 2003; Hladil et al., 2010). χ_{in} across the Silurian-Devonian boundary was extensively studied in eight sections including Požár-CS (Vacek et al., 2010). Its origin was evaluated by the temperature dependence of χ_{in}, magnetic hysteresis and Isothermal Remanent Magnetization (IRM) and by X-ray diffraction (Vacek et al., 2010). This study showed that the IRM data (determined by ferromagnetic minerals) are not correlated to magnetic susceptibility, indicating that the χ_{in} signal is mostly carried by paramagnetic minerals, with only minor influence of ferromagnetic minerals. Another detailed study of the χ_{in} record of the Požár-CS section, by optical microscopy, electron microprobe analysis and comparison of the χ_{in} records with those of GRS, $CaCO_3$ and Spectral Reflectance, led to similar conclusions, and in addition highlighted the small influence of pyrite, pyrrhotite, goethite and hematite (Koptíková et al., 2010b). Clear similarities between the χ_{in} and GRS records were highlighted by Koptíková et al. (2010a). This was confirmed in this work through the spectral analysis applied on both signals. Indeed, the same dominant frequencies and periods in both χ_{in} and GRS-Th and -K records were found in the wavelet and EHA of these records (Figs. 3–5 and A3–A4). GRS is reflecting the amount of clay minerals into the limestone and the similarity of the GRS and χ_{in} records indicates that the latter is not largely influenced by later detrimental diagnetic effects, i.e. creation of magnetite. This is also supported by hysteresis loop data (Fig. A5). Typical hysteresis loops from Pod Barrandovem are straight lines, with a positive or negative slope, indicating a magnetic susceptibility carried mostly by paramagnetic and diamagnetic minerals, with only a marginal influence of ferromagnetic minerals. In Požár-CS, hysteresis loops have mostly a negative high-field slope (diamagnetic) in the Lochkov Fm. and a positive slope (paramagnetic) in the Praha Fm. Furthermore, most of the loops also include a ferromagnetic component. The high field susceptibility (χ_{hf}) is influenced by the paramagnetic and diamagnetic minerals only; it correlates relatively well with χ_{in} ($r = 0.78$ in Pod Barrandovem and $r = 0.74$ in Požár-CS). The ferromagnetic susceptibility ($\chi_{ferro} = \chi_{in} - \chi_{hf}$) has slightly lower correlation coefficients with χ_{in} ($r = 0.56$ in Pod Barrandovem and $r = 0.67$ in Požár-CS). Pod Barrandovem shows best results (Figs. 4, A4) but

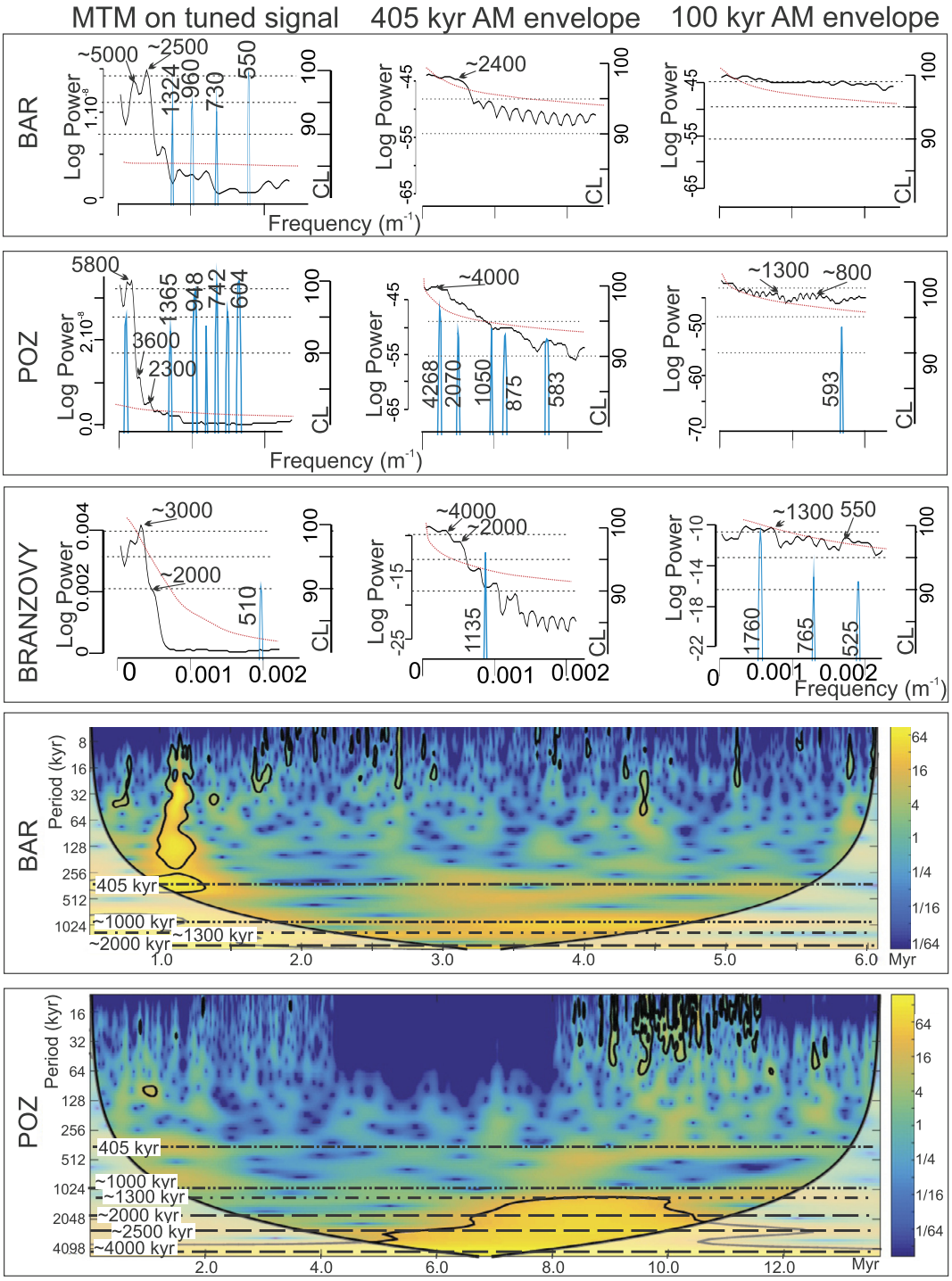

Fig. 6. Long-period orbital cycles in the Pod Barrandovem, Požár-CS and Branžovy sections. The upper part shows the MTM spectra (black line) and F-test (blue peaks) on the tuned χ_{in} records from Pod Barrandovem (BAR), Požár-CS (POZ) and Branžovy; as well as the MTM spectra and F-test of the 405 and 100 kyr tuned Amplitude envelope (AM) records. The lower part of the figure shows the CWT of the tuned records from Požár-CS and Pod Barrandovem. (For interpretation of the references to color in this figure, the reader is referred to the web version of this article.)

also in Požár-CS (Figs. 3, A3) the results are acceptable. In the latter the ferromagnetic contribution to χ_{in} is stronger, but the correlation between χ_{hf} and χ_{in} is still higher than that of χ_{ferro} and χ_{in}, which is a good indication that the clay minerals still carry the majority of the signal. All in all, this argues for a relatively low impact of diagenesis on our χ_{in} records, indicating that the χ_{in} and GRS signals are mainly carried by clay minerals reflecting paleoclimate information.

5.2. Recording of Milankovitch cycles and paleoenvironmental context

The next question is whether the sedimentary setting is appropriate for the recording of astronomically induced climate cycles, now that χ_{in} and GRS are considered as appropriate for their analysis. The studied sections are dominated by off-shore limestones, hemipelagites, with storm deposits and calciturbidites (Hladil et al., 2010). A turbiditic setting is classically considered to be domi-

nated by random depositional events, and as such, it would not be ideal to record orbital controlled cyclicity (Hinnov and Ogg, 2007).

Facies analysis of the Požár-CS section reveals that the Lochkov Fm. is dominated by hemipelagites, with the occasional occurrence of turbidites and subtidal deposits reworked by storms and/or bottom currents. The Praha Formation in Pod Barrandovem and Požár-CS sections appears to be dominated by very deep pelagic suspension deposits (Koptíková et al., 2010a). Therefore, the pelagic setting of the Praha Fm., is the most appropriate for recording the cyclicity. This would explain the enhanced spectral power bands in the CWT and EHA of the Praha Fm., compared to the weaker bands in the spectra of the Lochkov Fm. (Fig. 3).

It has been shown that turbiditic deposits can carry Milankovitch cyclicities, mostly in the context of an ice-house setting due to the amount of clastic sediments influenced by eccentricity and obliquity e.g. Droxler and Schlager (1985). The depositional setting from our sections, however, can be more appropriately compared with a greenhouse setting. An illustrative example is the Lutetian (Eocene) Gorrondatxe section (Western Pyrenees, Spain), that is dominated by basin turbiditic and pelagic limestones and marls. Payros and Martínez-Braceras (2014) performed a detailed study of the influence of orbital forcing in this turbiditic setting and demonstrated that turbiditic deposition can be orbitally controlled by terrestrial runoff and terrigeneous input into the basin. They link the increased turbiditic activity to strong seasonality and heavy summer rainfall. Approximately the same mechanism has been held responsible for turbiditic sequences associated with dominantly precession controlled organic-rich layers, termed sapropels, in the Mediterranean Miocene (Postma et al., 1993).

Turbidites can also lead to the distortion of the recording of the paleoenvironmental or paleoclimate information sought here, termed environmental shredding by Jerolmack and Paola (2010). In our case, environmental shredding does not seem to be an issue. Indeed, in Požár-CS and Pod Barrandovem sections, precession and obliquity are recorded in all intervals, except for the condensed intervals at 70.8–78 m and 112.8–118 m in Požár-CS where the sampling resolution is not sufficiently high. This implies that environmental shredding is not at a similar amplitude scale as precession and obliquity; therefore it does not interfere with the recording of these cycles.

In conclusion, the χ_{in} and GRS records from this pelagic/turbiditic setting can be used for cyclostratigraphic studies directed at improving the Early Devonian Time Scale. However, the recorded signal is not entirely pristine and not always straightforward. To provide the best possible interpretation we have combined various spectral analysis techniques, which should ideally be consistent to reinforce our final interpretation.

5.3. Astronomical time scale for the Lochkovian and Pragian

The duration of the different studied intervals is estimated through different approaches:

(1) combination of the thickness of each interval divided by its inferred SAR and
(2) by using the 405 kyr cycles (identified through EHA) as tie points to transfer the signal from the stratigraphic domain to the time domain (cf. section 3.4.).

Of course the two techniques should give similar results; however, the second is considered more precise because it takes into account minor SAR changes within the intervals of "steady" deposition.

5.3.1. Duration of the Lochkovian stage and the Lochkov formation

By comparing the outcome of the different spectral techniques, we obtained optimal SARs for the different intervals of the Lochkov Fm. and Lochkovian Stage (Fig. 3). By combining the SARs with the thickness of each interval, a duration of 7.6 Myr results for the Lochkovian and of 7.7 Myr for the Lochkov Fm. Alternatively, we obtained nineteen 405 kyr eccentricity cycles for the Lochkovian and for the Lochkov Fm. (Fig. 7, Table 2), corresponding to ~7.7 Myr. As mentioned before, the results from the tuning and 405 kyr cycle counting are considered as the most precise.

5.3.2. Duration of the Pragian stage and Praha formation

The total duration of the Pragian in the Požár-CS section calculated by applying the SAR obtained previously (Fig. 4) is of 1.75 Myr. With the same technique, we obtain a duration of 6.0 Myr for the Praha Fm. Alternatively, the Praha Fm. corresponds to fourteen 405 kyr eccentricity cycles and thus to a duration of 5.7 Myr, if we use the tuned filtered χ_{in} record in Požár-CS (Fig. 7, Table 2). For the Praha Fm. at Pod Barrandovem (Fig. 8), we need to include about 10 m of Slivenec limestone (the lowermost Praha Fm.) missing at the base of the section. This interval is considered to have the same SAR as the remainder of the Slivenec limestone in this section (0–12 m), and corresponding to about one 405 kyr eccentricity cycle. In total, the whole Praha Fm. at Pod Barrandovem also consists also of fourteen 405 kyr eccentricity cycles, including the extrapolated cycle that is missing at the base of the section. The Branžovy section (Fig. 5) also includes fourteen 405 kyr eccentricity cycles leading to a similar duration for the Praha Fm. in all three sections. This implies that there are likely no major gaps in any of the sections, as it would be very difficult to explain gaps of similar durations in different open marine settings.

5.4. Precision estimates

The uncertainties of the Early Devonian stages should be considered as over-optimistic, because of the adopted cubic spline-fitting approach used in the GTS-2012, which inherently underestimates the uncertainty (cf. discussion in De Vleeschouwer and Parnell, 2014). This applies in particular to cases as the Devonian, where only a few tie dates are available (Telford et al., 2004). This leads to an uncertainty which decreases with increasing stratigraphic distance from the radiometrically dated level, while more intuitively it should be the opposite. The duration of the Lochkovian and Pragian stages and their uncertainties calculated as such are 8.4 ± 3.5 Myr for the Lochkovian and 3.2 ± 1.2 Myr for the Pragian. The uncertainty calculated with error propagation (under the premise of independently determined upper and lower stage boundary uncertainties, Table 2) would give for the Lochkovian: 8.4 ± 4.25 Myr for the ages in Becker et al. (2012) and 7.7 ± 4.4 Myr for the ages in De Vleeschouwer and Parnell (2014). For the Pragian these are 3.2 ± 3.8 Myr for the Becker et al. (2012) data and 3.2 ± 4.3 for the De Vleeschouwer and Parnell (2014) data.

Uncertainty estimates for floating astronomical time scales are often not provided (e.g. Boulila et al., 2010; Ellwood et al., 2015), or the uncertainty is estimated by summing the uncertainty in the position of the lower and upper boundaries of a stage, combined with an uncertainty estimate of the cycle counting (e.g. De Vleeschouwer et al., 2012, 2015; Fang et al., 2015). In our case, the uncertainty in the position of the boundaries corresponds to the uncertainty in the position of lithological boundaries in case of the Formations and of conodont bio-event boundaries in case of the stages. The position of the Pridoli–Lochkovian stage boundary (i.e. the Silurian–Devonian boundary) is defined very precisely in the Požár-CS section and its uncertainty corresponds to a maximum error of ± 0.25 m. Combined with the inferred SAR for

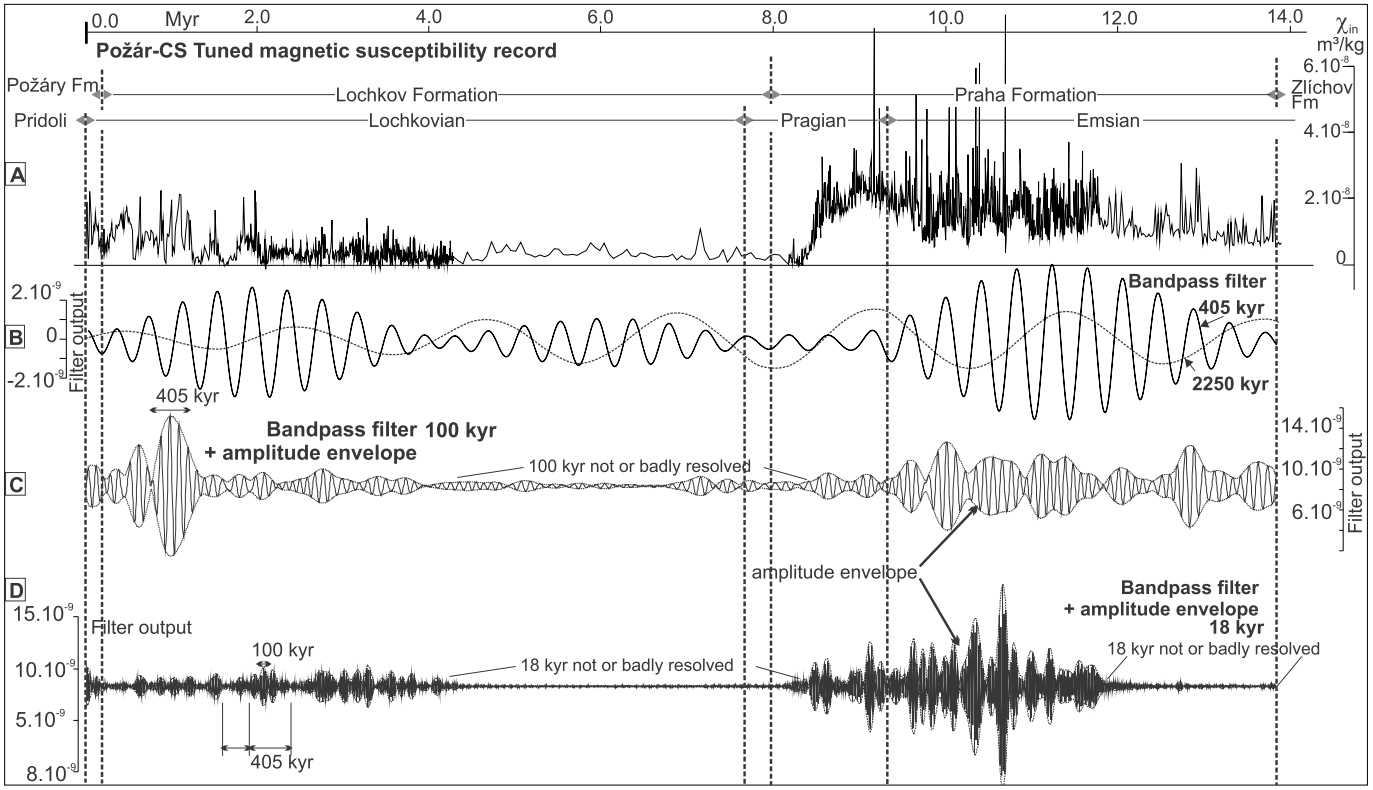

Fig. 7. Požár-CS section. Tuned χ_{in} record and its bandpass filter (405, 100 and 18 kyr filter). (A) Tuned (time scale) χ_{in} record. (B) Band-pass filtered tuned χ_{in} record at the 405-kyr (E1, 405 kyr eccentricity) and 2250 kyr cycles. (C) Band-pass filtered tuned χ_{in} record at 100-kyr cycles (E2, 100 kyr eccentricity) and amplitude envelope. This amplitude envelope appears to be modulated by the 405 kyr-cycles. (D) Band-pass filtered tuned χ_{in} record at 18-kyr cycles (precession) and its amplitude envelope (modulated by 100-kyr and 405-kyr).

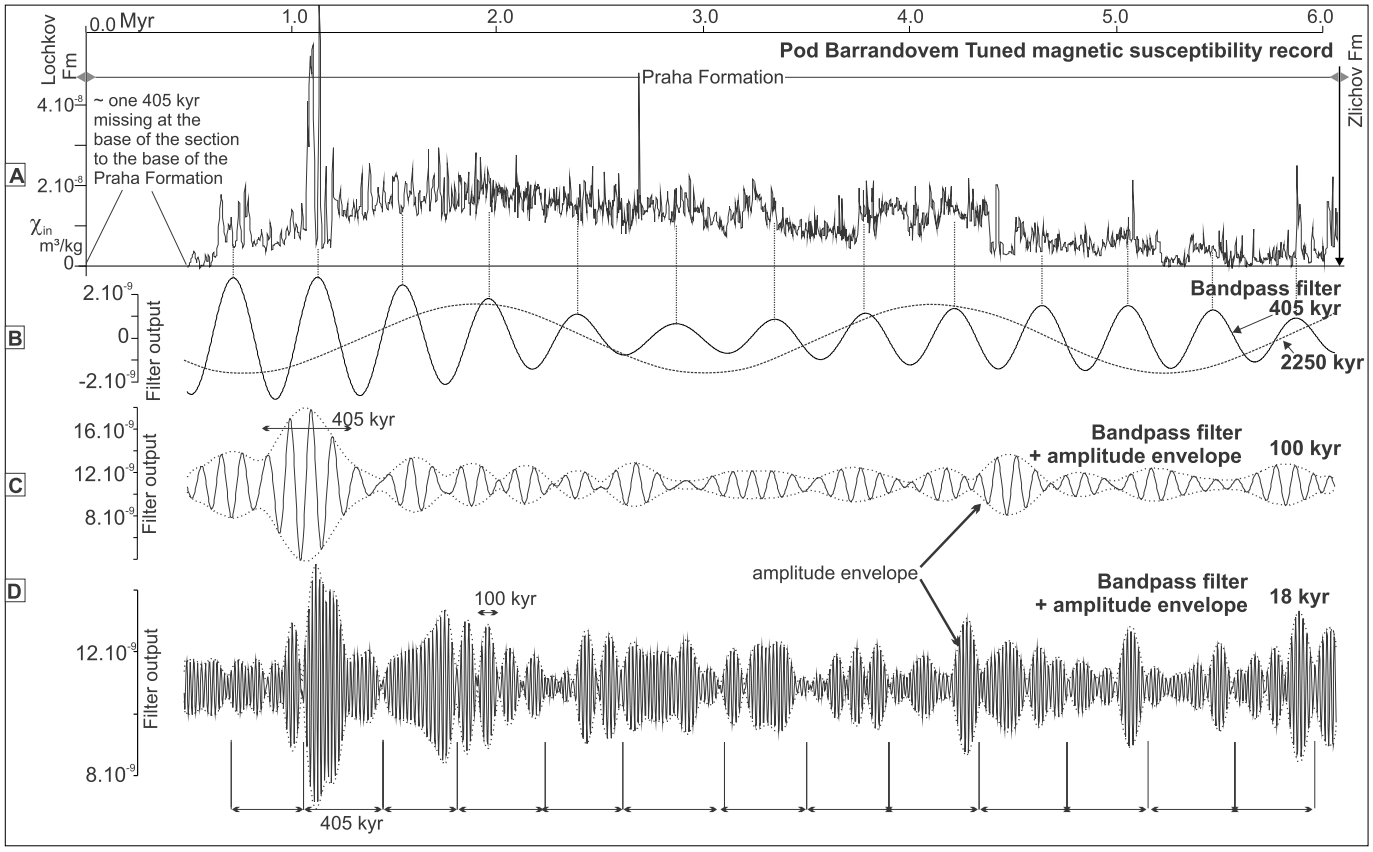

Fig. 8. Pod Barrandovem section. Tuned χ_{in} record and its bandpass filter (405, 100 and 18 kyr filter). Cf. caption to Fig. 7 for explanation.

the base of the section (1 cm/kyr), this corresponds to an uncertainty of ±0.03 Myr in the time domain (Table 2). For the Lochkovian–Pragian stage boundary (from the Požár-CS section), the uncertainty in the stratigraphic position is about ±0.55 m, corresponding to ±0.3 Myr, based on the SAR of 0.2 cm/kyr for that interval. The position of the Pragian–Emsian stage boundary (from the Požár-CS section) is very precise (±0.2 m, with a SAR of 0.9 cm/kyr) and corresponds to ±0.02 Myr. The positions of the Formation boundaries are lithologically very precisely pinpointed, with an uncertainty that corresponds to about ±0.2 m, equivalent to ±0.02 and ±0.1 Myr for the base and top of the Lochkov Fm. respectively, and to ±0.07 Myr for the top of the Praha Fm. (Table 2).

For the Lochkovian and Lochkov Fm. in the Požár-CS section, the uncertainty in the cycle count, however is unfortunately considered relatively high. Indeed, (1) the ASM results do not always match with the CWT and EHA results EHA, (2) only one section was analyzed without the possibility to check laterally equivalent sections for consistency, and (3) the low SAR (0.2 cm/kyr) inferred for the Upper Lochkovian is based only on the results of the ASM, it could not be confirmed by other techniques. The resulting low SAR potentially, carries large uncertainties with it in assessing the duration represented by the section. Therefore, we suggest a conservative uncertainty estimate of six 405 kyr cycles in the nineteen 405 kyr eccentricity cycles counted in the entire Lochkovian Stage and associated Lochkov Fm. The uncertainty from cycle counting and boundary position then results in a duration of 7.7 ± 2.6 Myr for the Lochkov Formation and 7.7 ± 2.8 Myr for the Lochkovian Stage (Table 2). This is comparable with the duration of the Lochkovian proposed by De Vleeschouwer and Parnell (2014; 7.7 ± 4.4 Myr) and Becker et al. (2012; 8.4 ± 4.25 Myr) but it is distinctly more precisely defined (by a factor 1.7, Table 2).

Concerning the uncertainty on the duration of the Pragian Stage and Praha Fm. (in the Požár-CS, Pod Barrandovem and Branžovy sections), we estimate an uncertainty of only one 405 kyr eccentricity in the cycle counting. This uncertainty was selected because: (1) the results of all spectral techniques are consistent, (2) ASM significance levels are excellent (Ho_SL ranging from 0.014% to 2.4%), and (3) results are reproducible for the three different parallel sections. This uncertainty, combined with the uncertainty in the position of the lower and upper boundaries results in a total duration of 5.7 ± 0.6 Myr for the Praha Fm. and of 1.7 ± 0.7 Myr for the Pragian Stage (Table 2). The latter duration is substantially shorter than the duration of the Pragian Stage proposed by De Vleeschouwer and Parnell (2014; 3.2 ± 4.3 or 5.5 Myr) and by Becker et al. (2012; 3.2 ± 3.8 Myr). In addition, our estimate comes with a markedly reduced uncertainty (Table 2), which is about 5 to 8 times lower than that of Becker et al. (2012) or De Vleeschouwer and Parnell (2014).

5.5. Amplitude modulation and long period orbital forcing during the Early Devonian

The influence of the different cycles and their long-term modulations can best be seen in the Pod Barrandovem section, which is the only section for which we were able to resolve the obliquity and precession related signals in all intervals and for all cycle types (Fig. 8b–8C). The different cycles were filtered from the tuned χ_{in} record. The bandpass filtered component of the 100 kyr eccentricity related signal, and its amplitude envelope calculated by means of the Hilbert Transform, is clearly modulated by the 405 kyr eccentricity cycle in groups of four 100 kyr cycles (Fig. 8C). In addition, the 18-kyr precession-related cycle amplitude envelope is modulated by both the 100 and 405 kyr eccentricity (Fig. 8D), as expected from astronomical theory. The tuning and filtering of the Požár-CS section also allows to detect the modulation of the 100 kyr eccentricity related cycles by the 405 kyr cycle, and of the 18 kyr cycles by the 100 and 405 kyr cyclicity (Fig. 7).

In addition to the well-known cycles of precession, and 100 and 405 kyr eccentricity cycles, modulation of these cycle components is also recorded and corresponds to lower frequency cycles. The main modulation of the 405 kyr eccentricity component today has a period of ~2400 kyr (classically known as the 2.4 Myr cycle; e.g. Laskar et al., 2011), and is also the one that is most often found in the geological record. Modulated cycles with periods of ~700 kyr, ~1000 kyr and 3500–4000 kyr cycles are present in the astronomical solution as well (Laskar et al., 2011). The period of the main 2400 kyr amplitude modulation cycle, may vary between 1200 and 2400 kyr as a consequence of the chaotic behavior of the Solar system (Laskar et al., 2011). The geological record indeed shows evidence of variations in the duration of this 2400 kyr cycle (see reviews in: Fang et al., 2015; Ikeda and Tada, 2013).

The main long-term cycles observed in our different records are around ~4000, 2500, 1300, ~1000 and ~700 kyr (Fig. 6). It is interesting to note that Lower-Middle Permian strata in South China yield spectral peaks around 4760, 1950, 1300, 1000 and 840 kyr (Fang et al., 2015) that are in the same range as those reported here. A ~2000–2500 kyr cycle, as well as amplitude modulations of the 405 and 100 kyr cycles, were all detected in all our tuned records (Fig. 6). Within the different records, a ~1000 kyr cycle is also consistently observed (Fig. 6), which can potentially be linked to the present-day ~1000 kyr eccentricity cycle, or the 1200 kyr amplitude modulation cycle of obliquity. The latter may also have evolved through time and appears to have been shorter in the Mesozoic and Palaeozoic (synthesis in Fang et al., 2015: ~1000 kyr in the Late Cretaceous, ~1000 kyr in the Permian and ~1120 kyr in the Late Devonian).

6. Conclusions

We obtained the following results by combining various spectral analysis or statistical techniques (Continuous Wavelet Transform, Evolutive Harmonic Analysis, Multi Taper Method combined with the Average Spectral Misfit) in the evaluation of χ_{in} and GRS records of three Lower Devonian sections in the Praha Synform (Czech Republic):

- The combination of different spectral and statistical techniques and records is very powerful and essential for carrying out a detailed cyclostratigrapic study of Devonian sections. It allows cross validation of results and rejection of weaker solutions in order to reach the best possible interpretation and construct an optimal age model.
- The χ_{in} and GRS records from a (hemi-)pelagic and turbiditic setting yielded consistent results. This points to a similar origin for both proxies, with the signal residing in clay minerals and reflecting climatic variations.
- The new age model results in durations of 7.7 ± 2.6 Myr for the Lochkov Fm., of 7.7 ± 2.8 Myr for the Lochkovian Stage, 5.7 ± 0.6 Myr for the Praha Fm. and of 1.7 ± 0.7 Myr for the Pragian Stage. Because the Lochkov Fm./Lochkovian contains an interval with a very low sediment accumulation rate and because these results were only derived from one section, the uncertainty of its duration is larger than that of the Praha Fm. and Pragian (cross-validated over three sections). The application of this cyclostratigraphic approach leads to a reduction of the uncertainty for Early Devonian Time Scale by a factor of 1.7 for the duration of the Lochkovian Stage and by a factor of 5 to 8 for the Pragian Stage, compared to most recent time scales;
- Very long period cycles have also been identified in the three sections, namely a ~2000–2500 kyr cycle interpreted to reflect

long-term eccentricity amplitude modulation and a ~1000 kyr cycle interpreted as an amplitude modulation cycle of obliquity.

Acknowledgements

This research project was supported by the Netherlands Organization for Scientific Research (NWO, grant WE.210012.1) and the Czech Science Foundation (GAČR), research project 14-18183S "sequence stratigraphy of Devonian bioevents – sea level changes at the transition from greenhouse to icehouse world". Thanks to D. De Vleeschouwer for inspiring discussions over spectral analysis applied on Palaeozoic sediments. We would like to thank Martin Frank, the EPSL editor and K. Kodama and anonymous reviewer for comments that helped to improve the manuscript.

Appendix A. Supplementary material

Supplementary material related to this article can be found online at http://dx.doi.org/10.1016/j.epsl.2016.09.009.

References

Arculus, R.J., Ishizuka, O., Bogus, K., the E. 351 S., 2015. Expedition 351 summary. In: Proceedings of the International Ocean Discovery Program, vol. 351, pp. 1–25.

Bábek, O., Kalvoda, J., Cossey, P., Šimíček, D., Devuyst, F.-X., Hargreaves, S., 2013. Facies and petrophysical signature of the Tournaisian/Viséan (Lower Carboniferous) sea-level cycle in carbonate ramp to basinal settings of the Wales–Brabant massif, British Isles. Sediment. Geol. 284–285, 197–213. http://dx.doi.org/10.1016/j.sedgeo.2012.12.008.

Bábek, O., Kumpan, T., Kalvoda, J., Matys Grygar, T., 2016. Devonian/Carboniferous boundary glacioeustatic fluctuations in a platform-to-basin direction: a geochemical approach of sequence stratigraphy in pelagic settings. Sediment. Geol. 337, 81–99. http://dx.doi.org/10.1016/j.sedgeo.2016.03.009.

Becker, R.T., Gradstein, F.M., Hammer, O., 2012. The Devonian period. In: Gradstein, F.M., Ogg, J.G., Schmitz, M.D., Ogg, G.M. (Eds.), The Geologic Time Scale 2012. Elsevier B.V., pp. 559–602.

Berger, A., Loutre, M.F., Laskar, J., 1992. Stability of astronomical frequencies over the Earth's history for paleoclimate studies. Science 255, 560–566.

Boulila, S., Galbrun, B., Hinnov, L.A., Collin, P.Y., Ogg, J.G., Fortwengler, D., Marchand, D., 2010. Milankovitch and sub-Milankovitch forcing of the Oxfordian (Late Jurassic) Terres Noires Formation (SE France) and global implications. Basin Res. 22, 717–732. http://dx.doi.org/10.1111/j.1365-2117.2009.00429.x.

Carls, P., Slavík, L., Valenzuela-Ríos, J.I., 2008. Comments on the GSSP for the basal Emsian stage boundary: the need for its redefinition. Bull. Geosci. 83 (4), 383–390.

Chlupáč, I., 2000. Cyclicity and duration of Lower Devonian stages: observations from the Barrandian area, Czech Republic. Neues Jahrb. Geol. Paläontol. Abh. 215, 97–124.

Chlupáč, I., Havlicek, V., Kriz, J., Kukal, Z., Storch, P., 1998. Palaeozoic of the Barrandian (Cambrian to Devonian). Czech Geological Survey. 183 pp.

Da Silva, A.-C., Dekkers, M.J., Mabille, C., Boulvain, F., 2012. Magnetic susceptibility and its relationship with paleoenvironments, diagenesis and remagnetization: examples from the Devonian carbonates of Belgium. Stud. Geophys. Geod. 56, 677–704. http://dx.doi.org/10.1007/s11200-011-9005-9.

Da Silva, A.-C., De Vleeschouwer, D., Boulvain, F., Claeys, P., Fagel, N., Humblet, M., Mabille, C., Michel, J., Sardar Abadi, M., Pas, D., Dekkers, M.J.J., 2013. Magnetic susceptibility as a high-resolution correlation tool and as a climatic proxy in Paleozoic rocks – merits and pitfalls: examples from the Devonian in Belgium. Mar. Pet. Geol. 46, 173–189. http://dx.doi.org/10.1016/j.marpetgeo.2013.06.012.

De Vleeschouwer, D., Parnell, A.C., 2014. Reducing time-scale uncertainty for the Devonian by integrating astrochronology and Bayesian statistics. Geology 42, 491–494. http://dx.doi.org/10.1130/G35618.1.

De Vleeschouwer, D., Boulvain, F., Da Silva, A.-C., Pas, D., Labaye, C., Claeys, P., 2015. The astronomical calibration of the Givetian (Middle Devonian) timescale (Dinant Synclinorium, Belgium). Geol. Soc. (Lond.) Spec. Publ. 414, 25–37. http://dx.doi.org/10.1144/SP414.3.

De Vleeschouwer, D., Rakociński, M., Racki, G., Bond, D.P.G., Sobień, K., Claeys, P., 2013. The astronomical rhythm of Late-Devonian climate change (Kowala section, Holy Cross Mountains, Poland). Earth Planet. Sci. Lett. 365, 25–37. http://dx.doi.org/10.1016/j.epsl.2013.01.016.

De Vleeschouwer, D., Whalen, M.T., Day, J.E., Claeys, P., 2012. Cyclostratigraphic calibration of the Frasnian (Late Devonian) time-scale (Western Alberta, Canada). Geol. Soc. Am. Bull. 124, 928–942.

Droxler, A.W., Schlager, W., 1985. Glacial versus interglacial sedimentation rates and turbidite frequency in the Bahamas. Geology 13, 799–802.

Ellwood, B.B., El Hassani, A., Tomkin, J.H., Bultynck, P., 2015. A climate-driven model using time-series analysis of magnetic susceptibility (χ) datasets to represent a floating-point high-resolution geological timescale for the Middle Devonian Eifelian stage. Geol. Soc. (Lond.) Spec. Publ. 414, 209–223. http://dx.doi.org/10.1144/SP414.4.

Fang, Q., Wu, H., Hinnov, L.A., Jing, X., Wang, X., Jiang, Q., 2015. Geologic evidence for chaotic behavior of the planets and its constraints on the third-order eustatic sequences at the end of the Late Paleozoic Ice Age. Palaeogeogr. Palaeoclimatol. Palaeoecol. 440, 848–859. http://dx.doi.org/10.1016/j.palaeo.2015.10.014.

Grabowski, J., Bábek, O., Nawrocki, J., Tomek, Č., 2010. New palaeomagnetic data from the Palaeozoic carbonates of the Moravo-Silesian Zone (Czech Republic): evidence for a timing and origin of the late Variscan remagnetization. Geol. Q. 52, 321–334.

Hilgen, F.J., Lourens, L.J., Van Dam, J.A., Beu, A.G., Boyes, A.F., Cooper, R.A., Krijgsman, W., Ogg, J.G., Piller, W.E., Wilson, D.S., 2012. The Neogene period. In: Gradstein, F.M., Ogg, J.G., Schmitz, M.D., Ogg, G.M. (Eds.), The Geologic Time Scale. Elsevier, pp. 923–978.

Hinnov, L.A., Ogg, J.G., 2007. Cyclostratigraphy and the astronomical time scale. Stratigraphy 4, 239–251.

Hinnov, L., Kodama, K.P., Anastasio, D.J., Elrick, M., Latta, D.K., 2013. Global Milankovitch cycles recorded in rock magnetism of the shallow marine lower Cretaceous Cupido Formation, northeastern Mexico. In: Jovane, L., Herrero-Bervera, E., Hinnov, L. (Eds.), Magnetic Methods and the Timing of Geological Processes. Geol. Soc. (Lond.) Spec. Publ. 373, 325–340.

Hladil, J., Vondra, M., Cejchan, P., Vich, R., Koptíková, L., Slavík, L., 2010. The dynamic time-warping approach to comparison of magnetic-susceptibility logs and application to lower Devonian calciturbidites (Prague Synform, Bohemian Massif). Geol. Belg. 13, 385–406.

Hladil, J., Slavík, L., Vondra, M., Koptíková, L., Cejchan, P., Schnabl, P., Adamovic, J., Vacek, F., Vich, R., Lisa, L., Lisy, P., 2011. Pragian–Emsian successions in Uzbekistan and Bohemia: magnetic susceptibility logs and their dynamic time warping alignment. Stratigraphy 8 (4), 217–235.

Ikeda, M., Tada, R., 2013. Long period astronomical cycles from the Triassic to Jurassic bedded chert sequence. (Inuyama, Japan); geologic evidences for the chaotic behavior of solar planets. Earth Planets Space 65, 351–360. http://dx.doi.org/10.5047/eps.2012.09.004.

Jerolmack, D.J., Paola, C., 2010. Shredding of environmental signals by sediment transport. Geophys. Res. Lett. 37. http://dx.doi.org/10.1029/2010GL044638.

Joachimski, M.M., Breisig, S., Buggisch, W., Talent, J.A., Mawson, R., Gereke, M., Morrow, J.R., Day, J., Weddige, K., 2009. Devonian climate and reef evolution: insights from oxygen isotopes in apatite. Earth Planet. Sci. Lett. 284, 599–609. http://dx.doi.org/10.1016/j.epsl.2009.05.028.

Kodama, K.P., Hinnov, L.A., 2015. Rock Magnetic Cyclostratigraphy. John Wiley & Sons, Ltd., p. 165.

Kodama, K.P., Anastasio, D.J., Newton, M.L., Pares, J.M., Hinnov, L.A., 2010. High-resolution rock magnetic cyclostratigraphy in an Eocene flysch, Spanish Pyrenees. Geochem. Geophys. Geosyst. 11. http://dx.doi.org/10.1029/2010GC003069.

Koptíková, L., Bábek, O., Hladil, J., Kalvoda, J., Slavík, L., 2010a. Stratigraphic significance and resolution of spectral reflectance logs in Lower Devonian carbonates of the Barrandian area, Czech Republic; a correlation with magnetic susceptibility and gamma-ray logs. Sediment. Geol. 225, 83–98. http://dx.doi.org/10.1016/j.sedgeo.2010.01.004.

Koptíková, L., Hladil, J., Slavík, L., Čejchan, P., Bábek, O., 2010b. Fine-grained non-carbonate particles embedded in neritic to pelagic limestones (Lochkovian to Emsian, Prague Synform, Czech Republic): composition, provenance and links to magnetic susceptibility and gamma-ray logs. Geol. Belg. 13, 407–430.

Krs, M., Pruner, P., Man, O., 2001. Tectonic and paleogeographic interpretation of the paleomagnetism of Variscan and pre-Variscan formations of the Bohemian Massif, with special reference to the Barrandian terrane. Tectonophysics 332, 93–114.

Laskar, J., Fienga, A., Gastineau, M., Manche, H., 2011. La2010: a new orbital solution for the long term motion of the Earth. Astron. Astrophys. 532, 15. http://dx.doi.org/10.1051/0004-6361/201116836.

Mayer, H., Appel, E., 1999. Milankovitch cyclicity and rock-magnetic signatures of palaeoclimatic change in the Early Cretaceous Biancone Formation of the Southern Alps, Italy. Cretac. Res. 20, 189–214. http://dx.doi.org/10.1006/cres.1999.0145.

Meyers, S.R., 2014. Astrochron: an R package for astrochronology. Version 0.3.1.

Meyers, S.R., Sageman, B.B., 2007. Quantification of deep-time orbital forcing by average spectral misfit. Am. J. Sci. 307, 773–792.

Meyers, S.R., Sageman, B.B., Hinnov, L.A., 2001. Integrated quantitative stratigraphy of the Cenomanian–Turonian bridge Creek Limestone member using evolutive harmonic analysis and stratigraphic modeling. J. Sediment. Res. 71, 628–644. http://dx.doi.org/10.1306/012401710628.

Meyers, S.R., Sageman, B.B., Pagani, M., 2008. Resolving Milankovitch: consideration of signal and noise. Am. J. Sci. 308, 770–786. http://dx.doi.org/10.2475/06.2008.02.

Payros, A., Martínez-Braceras, N., 2014. Orbital forcing in turbidite accumulation during the Eocene greenhouse interval. Sedimentology 61, 1411–1432. http://dx.doi.org/10.1111/sed.12113.

Postma, G., Hilgen, F.J., Zachariasse, W.J., 1993. Precession-punctuated growth of a late Miocene submarine-fan lobe on Gavdos (Greece). Terra Nova 5, 438–444.

Plusquellec, Y., Hladil, J., 1998. Tabulate corals of Ibarmaghian affinities in the uppermost Emsian of Bohemia. Geol. Palaeontol. 35, 31–51.

Riquier, L., Averbuch, O., Devleeschouwer, X., Tribovillard, N., 2010. Diagenetic versus detrital origin of the magnetic susceptibility variations in some carbonate Frasnian–Famennian boundary sections from Northern Africa and Western Europe: implications for paleoenvironmental reconstructions. Int. J. Earth Sci. 99, S57–S73.

SDS Newsletter, 2014. Subcommission of Devonian stratigraphy. Newsletter 29, edited by Becker, T.R., available at http://unica2.unica.it/sds/.

Slavík, L., 2004a. A new conodont zonation of the Pragian in the stratotype area (Barrandian, central Bohemia). Newsl. Stratigr. 40, 39–71.

Slavík, L., 2004b. The Pragian–Emsian conodont successions of the Barrandian area: search of an alternative to the GSSP polygnathid-based correlation concept. Geobios 37, 454–470.

Slavík, L., Carls, P., Hladil, J., Koptíková, L., 2012. Subdivision of the Lochkovian Stage based on conodont faunas from the stratotype area (Prague Synform, Czech Republic). Geol. J. 47, 616–631. http://dx.doi.org/10.1002/gj.2420.

Slavík, L., Valenzuela-Ríos, J.I., Hladil, J., Carls, P., 2007. Early Pragian conodont-based correlations between the Barrandian area and the Spanish Central Pyrenees. Geol. J. 42, 499–512. http://dx.doi.org/10.1002/gj.1087.

Slavík, L., Valenzuela-Ríos, J.I., Hladil, J., Chadimová, L., Liao, J.-C., Hušková, A., Calvo, H., Hrstka, T., 2016. Warming or cooling in the Pragian? Sedimentary record and petrophysical logs across the Lochkovian–Pragian boundary in the Spanish Central Pyrenees. Palaeogeogr. Palaeoclimatol. Palaeoecol. 449, 300–320. http://dx.doi.org/10.1016/j.palaeo.2016.02.018.

Telford, R., Heegaard, E., Birks, H., 2004. All age-depth models are wrong: but how badly? Quat. Sci. Rev. 23, 1–5. http://dx.doi.org/10.1016/j.quascirev.2003.11.003.

Thomson, D.J., 1982. Spectrum estimation and harmonic analysis. Proc. IEEE 70, 1055–1096. http://dx.doi.org/10.1109/PROC.1982.12433.

Torrence, C., Compo, G.P., 1998. A practical guide to wavelet analysis. Bull. Am. Meteorol. Soc. 79, 61–78. http://dx.doi.org/10.1175/1520-0477(1998)079<0061:apgtwa>2.0.co;2.

Vacek, F., Hladil, J., Schnabl, P., 2010. Stratigraphic correlation potential of magnetic susceptibility and gamma-ray spectrometric variations in calciturbiditic facies mosaics (Silurian–Devonian boundary, Barrandian area, Czech Republic). Geol. Carpath. 61, 257–272.

Zwing, A., 2003. Causes and mechanisms of remagnetisation in Palaeozoic sedimentary rocks – a multidisciplinary approach. PhD thesis. Ludwig Maximilian's University of Munich. 159 pp.